NJC

Cite this: *New J. Chem.*, 2011, **35**, 156–164

www.rsc.org/njc

PAPER

X-Ray crystallographic and spectroscopic properties of eight Schiff bases as evidence of the proton transfer reaction. Role of the intermolecular hydrogen bond†

Oscar Domínguez,[a] Braulio Rodríguez-Molina,[a] Mario Rodríguez,[b] Armando Ariza,[a] Norberto Farfán[c] and Rosa Santillan*[a]

Received (in Gainesville, FL, USA) 6th March 2010, Accepted 4th September 2010
DOI: 10.1039/c0nj00179a

A spectroscopic study of several *ortho*-hydroxy Schiff bases was carried out, and the corresponding crystal structures were analyzed in order to identify their characteristic hydrogen bonding patterns. The X-ray analysis showed that the enol (O–H···N) tautomer is the most stable in compounds **1–3** whereas the keto (N–H···O) form is preferred in compounds **4–7**. The specific intermolecular O–H···O hydrogen bonding interactions that control the supramolecular arrangement of each tautomer are discussed. Additionally, a complete characterization of the polycrystalline samples was attained using solid-state NMR and IR experiments. Solution VT NMR and UV-visible experiments were also used to obtain valuable insights about the nature and stability of the tautomers.

Introduction

Schiff bases are important organic compounds of successful application in several areas, such as biological chemistry[1] materials science[2] and organic synthesis.[3] A tautomeric equilibrium between the enol O–H···N and keto N–H···O forms is commonly present in derivatives of aromatic-*o*-hydroxyaldehydes. A reversible intramolecular proton transfer driven by electrostatic differences between the oxygen and nitrogen atoms of the salicylideneimine fragment promotes the delocalization of the aromatic π-electron system leading to a quinoid form, which is also related with its canonical zwitterionic form[4] (Scheme 1).

Furthermore, it has been described that this tautomerism can be suitably controlled in the solid state by using light or temperature, depending on the photo- or thermochromic properties of the molecules,[5] making these compounds potential candidates for optical switches and storage devices.[6]

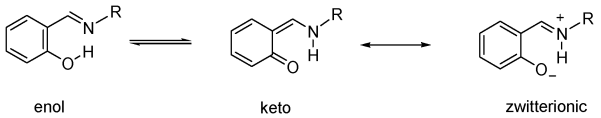

Scheme 1 Tautomeric equilibrium for arylimine derivatives.

Although extensive studies of several Schiff bases have been carried out, most of them are related with the synthesis and spectroscopic characterization of the tautomers,[7] or merely focused on simple structural description of the crystal structures.[8] Moreover, although the tautomeric equilibrium of the Schiff bases in solution has been widely explored,[9] studies concerning the factors that determine the formation of the tautomers in the solid-state are scarce.[10]

A preliminary work by Ogawa *et al.* provided the first X-ray evidence of the effects of the intermolecular contacts on the stabilization of the keto tautomers in salicylideneimine derivatives.[12] Subsequently, he showed that the proton transfer reaction in nonpolar solvents might be controlled by the aggregation state of the molecules at low temperatures[13] (Scheme 2).

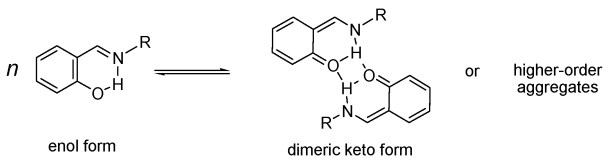

Scheme 2 Intramolecular cyclic dimer that stabilizes keto tautomers in solution.

[a] *Departamento de Química, Centro de Investigación y de Estudios Avanzados del IPN, CINVESTAV, Apdo., Postal 14-740, México, D. F., 07000, México. E-mail: rsantill@cinvestav.mx; Fax: +52 555-747-3389; Tel: +52 555-747-3725*
[b] *Centro de Investigaciones en Óptica, CIO, Apdo., Postal 1-948, 37000 León Gto., México*
[c] *Facultad de Química, Departamento de Química Orgánica, Universidad Nacional Autónoma de México, México, D.F., 04510, México*

† Electronic supplementary information (ESI) available: NMR characterization and experimental procedures for the preparation of all compounds, figure with high temperature VT NMR data of compound **5** in DMSO-d_6, table with a complete list of intra- and intermolecular contacts, additional figure for the crystal packing of compound **7**. CCDC reference numbers 712147 (**1**), 712151 (**2**), 712153 (**3**), 712149 (**4**) 712150 (**5**), 712154 (**6**), 712155 (**7**) and 712152 (**8**). For ESI and crystallographic data in CIF or other electronic format see DOI: 10.1039/c0nj00179a

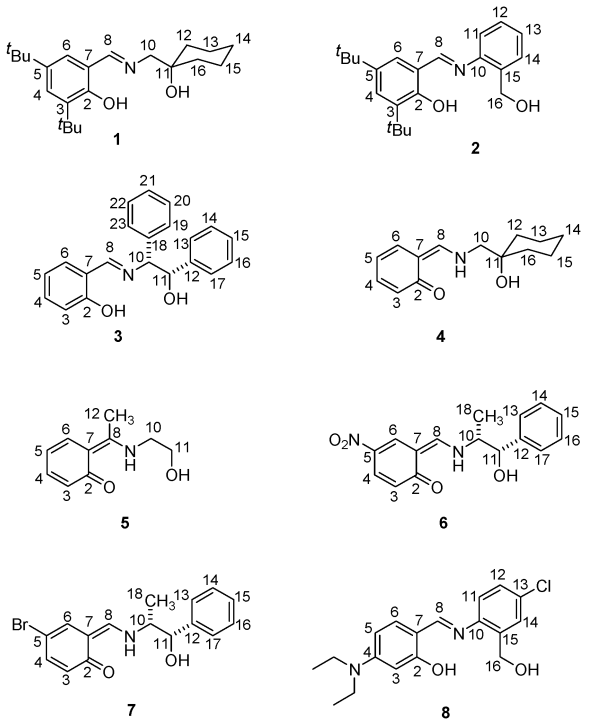

Scheme 3 Molecular structures of the Schiff bases studied. Compounds are depicted as observed in X-ray diffraction. For compound **8** the enol tautomer is depicted.

In a previous paper, we reviewed the stabilizing effect of intermolecular contacts of keto forms of imine derivatives from salicylaldehyde and substituted anilines.[11] In this work, we extended the investigation to eight *ortho*-hydroxy Schiff bases to unveil the influence (electronic and/or structural) of the substituents on the tautomeric structure from a crystallographic perspective (Scheme 3). In the selection of substituents were considered weak or good electron donors as tert-butyl and diethylamine groups, and electron withdrawing substituents such as, $-NO_2$, and other groups like –Cl and –Br, to explore the acidity of the salicylidene fragment in the proton transfer process. Furthermore, large groups as diphenyl or *t*-butyl groups were introduced to evaluate the influence of the steric effect on the tautomerism.

Besides the intramolecular hydrogen bonds present in the salicylidene fragment, the X-ray diffraction analysis revealed the existence of five specific intermolecular hydrogen-bonding patterns due to well aligned O–H···O hydrogen bonds: zigzag chains (compound **1**, Scheme 4a), tetrameric rings (imine **2**, Scheme 4b), linear chains (compounds **3–4**, Scheme 4c), helical chains (derivative **5**, Scheme 4d), cyclic dimeric rings (compounds **6–7**, Scheme 4e) or more complex arrangements such as those observed in compound **8** (Fig. 5).

Complementary UV-visible and solution NMR experiments supplied valuable insights about the tautomerization of these compounds and proved that the main attained form in solution is not directly related with that obtained in the solid-state, where the tautomeric stabilization is completely dependent on the prevailing contributions in the liquid phase (dipoles moments, solvation effects, molecular

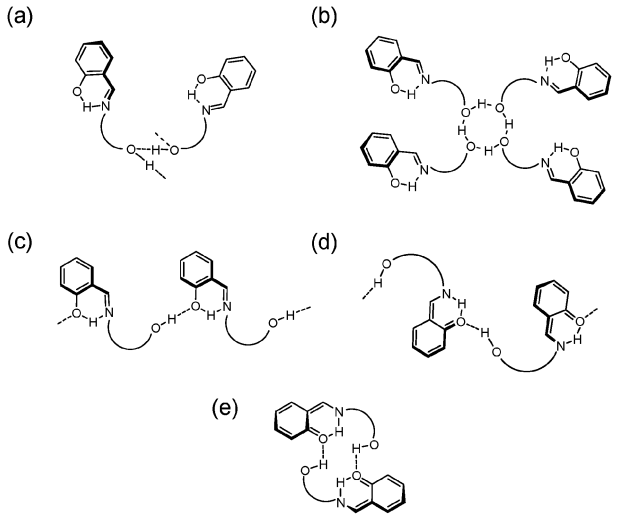

Scheme 4 Intermolecular interactions observed in imine derivatives.

aggregates, *etc.*)[10a,14] or in the solid phase (structural and electronic effects, hydrogen-bonding, *etc.*).[15]

Results and discussion

Characterization of compounds 1–8 in solution

Compounds **1–8** were prepared from the condensation reaction in methanol of different aminoalcohols and the corresponding salicylaldehyde. An important aspect of these compounds is the introduction of a complementary hydroxyl group, pertaining to the aminoalcohol unit labeled (O2–H2), in addition to the corresponding OH-salicylidene group marked as (O1–H1) that may confer additional stability to the supramolecular structures of all derivatives by establishing complementary interactions. In derivatives **2** and **8**, the hydrogen-bonding interactions among neighboring molecules are additionally strengthened by minimization of the steric repulsions.[15]

The use of absorption spectroscopy (UV-vis) for the identification of tautomeric species in solution[16] has permitted to propose that the formation of intermolecular hydrogen-bonded aggregates at low temperature stabilizes the keto forms in nonpolar solvents[13] (Scheme 2), even though the structure of these aggregates has not been clearly determined. In order to characterize the behavior of compounds **1–8** in solution, we measured the absorption spectra in different solvents at room temperature. Fig. 1 contains the spectra of compounds **4** and **5**.

In polar-protic solvents (methanol and ethanol) the keto tautomer (λ_{max} = 400 nm) was considerably formed in compound **4**, although the enol species (λ_{max} = 320 nm) remained preferentially stabilized.[21] Conversely, the intensity of the absorption bands indicated that the keto tautomer was slightly favored in methanol and ethanol for the derivative **5** even though a significant amount of the enol form was detected. In addition, in aprotic solvents as toluene and dimethylformamide, both compounds were predominantly stabilized in their enol form (λ_{max} = 320 nm) with a band

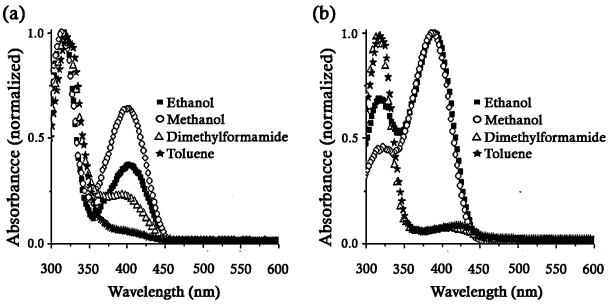

Fig. 1 UV-Vis spectra of compounds (a) **4** and (b) **5** in solvents of different polarity at room temperature. The bands at 320 and 400 nm are attributed to the enol and keto forms, respectively.

of much less intensity corresponding to the keto form (λ_{max} = 400 nm) also observed.[16b,c]

The spectral data showed that the keto form is moderately enhanced by protic-polar solvents and much less favored in aprotic ones. This evidence suggests that the characterization of the Schiff bases **1–8** in $CDCl_3$ solution (see ESI†) corresponds to an averaged structure (zwitterionic)[7a] from contributions of their enol and the keto species established in function of the nature of the solvent,[14a–c,17] which seems a recurrent phenomenon in the solution NMR characterization of related compounds.[7a]

We investigated further the equilibrium in solution taking advantage of the structural simplicity of compounds **4–5**, where a zwitterionic character is assumed in solution. It is well known that the ^{1}H-chemical shift of the salicylidene OH signal of the Schiff bases is strongly dependent on their tautomeric structures[18] with highly shifted signals being related to the keto character. In this series of compounds the salicylidene OH-chemical shift in $CDCl_3$ was in the range from 13.18 to 16.75 ppm. Accordingly, ^{13}C NMR spectra of all compounds showed the resonances corresponding to the salicylidene C2 atoms ranging from 160.5 to 173.7 ppm at room temperature. Therefore, we performed a solution VT NMR study of these compounds to investigate the effect of the solvent over the proton transfer process as a function of temperature[10a,19] in the temperature range from 200 to 400 K.

With regard to compound **4** (Fig. 2a), the salicylidene OH signal reached the maximum chemical shift at the lowest temperature, indicating that the intramolecular hydrogen bond (O–H···N / N–H···O) is evidently strengthened.[20] Conversely, this signal was shifted to lower frequencies at room temperature. These data reveals that the zwitterionic character of **4** is increasingly shifted toward its keto form as the temperature is decreased.[10a,19] Evidently, the solvent also contributes to the stabilization of the keto forms,[9c] since the highest OH-chemical shift was observed in the solvent with the highest polarity (DMF-d_7) as compared to CD_2Cl_2. This effect is based on the better stabilization of the keto form through electrostatic interactions (Scheme 1) as has been demonstrated by experimental and theoretical studies.[10a,b,21]

As we have previously pointed out, the salicylideneimine compounds in solution are generally best described as their averaged tautomeric forms at room temperature. However,

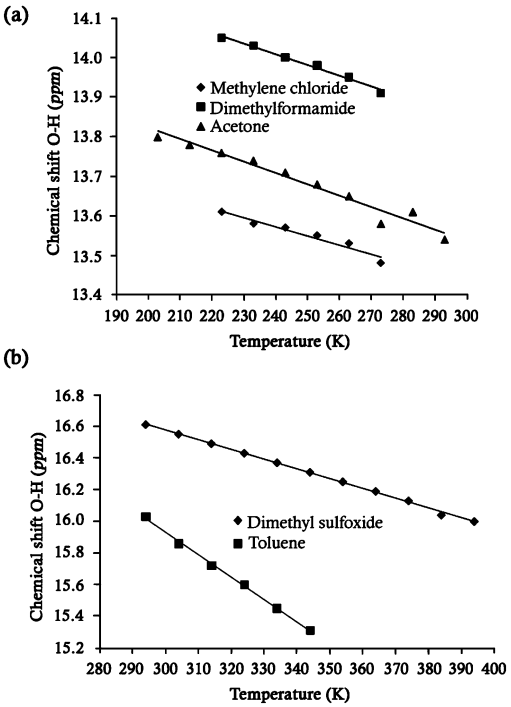

Fig. 2 ^{1}H VT NMR data for the OH signals in different solvents: (a) compound **4** and (b) compound **5**.

the ^{1}H and ^{13}C spectra of compound **5** in $CDCl_3$ at room temperature showed signals at 16.75 and 166.9 ppm for the salicylidene OH and C2 atoms, respectively, which are characteristic of derivatives with a marked keto character.[14c,19c] For this reason, compound **5** also was studied by VT NMR experiments using toluene-d_8 and DMSO-d_6. As expected, above room temperature the tautomeric equilibrium shifts towards the enol form. A shift of the salicylidene OH signal to low fequencies was observed as the temperature was increased (Fig. 2b), in accordance with the weakening effect of the temperature on the intramolecular hydrogen-bonding.[22] Unfortunately, heating the imine **5** above 344 K in DMSO-d_6 promotes a continuous hydrolysis that reaches a 15% ratio of hydrolyzed product at 394 K (see ESI†). The effect of the temperature in pyridine-d_5 was also tested but the results showed no clear relation with the OH-chemical shift, due to the competition between the pyridine (solvent) and the imine nitrogen atom (compound **5**) for the mobile proton.

Characterization in the solid-state of compounds 1–8

The IR analysis of crystalline compounds **1–8** obtained from methanol gave the first indication of the tautomeric form present. Characteristic bands were assigned in accordance with the literature data.[23] Compounds **1–3** showed a sharp band around 3441–3316 cm^{-1} due to the ν(OH) vibration, whereas compounds **4–7** present a broad band assignable to the ν(NH) vibration around 3214–3053 cm^{-1}. These data indicate the keto character of compounds **4–7** and the enol form in compounds **1–3**. Bands for the C=N bonds are in the range of 1627 to 1614 cm^{-1} in enol tautomers, while band for C=O bonds in the keto species range from 1657 to 1639 cm^{-1}.

In the case of compound **8** the IR spectrum suggested the presence of both tautomeric species showing broad bands in all regions of the spectrum. Two bands above 3212 cm^{-1} may correspond to O–H···N, N–H···O and/or O–H···O interactions, and a very broad band at 1600 cm^{-1} can be attributed to the concomitant C═O and C═N bonds of keto and enol tautomers. X-Ray experiments confirmed the presence of both forms in the crystal of compound **8**, as described in a further section.

X-Ray diffraction studies of compounds 1–7

After the initial experiments in solution, a detailed analysis of the molecular and packing motifs was carried out. Suitable crystals for X-ray diffraction[24] of all compounds (**1–8**) were grown by slow evaporation of the methanolic solutions at room temperature. The most relevant crystallographic parameters are shown in Tables 1 and 2.

Compounds **1** and **5** crystallize in the monoclinic space group $P2_1/c$ containing eight and four molecules per unit cell, respectively. Compounds **3** and **4** crystallize in the orthorhombic space groups $P2_12_12_1$ and $Pca2_1$, respectively, with four molecules per unit cell. Finally, compounds **2**, **6** and **7** crystallize in the triclinic system, with four molecules per unit cell in the imine **2** ($P\bar{1}$), and two crystallographically independent molecules in the imines **6** and **7** ($P1$).

Table 1 Selected crystal and refinement data for compounds **1–4**

Crystal data[a]	**1**	**2**[d]	**3**	**4**
Formula	$C_{22}H_{35}NO_2$	$C_{22}H_{29}NO_2$	$C_{21}H_{19}NO_2$	$C_{14}H_{19}NO_2$
MW/g mol^{-1}	345.51	339.46	317.37	233.30
Crystal system	Monoclinic	Triclinic	Orthorhombic	Orthorhombic
Space group	$P2_1/c$	$P\bar{1}$	$P2_12_12_1$	$Pca2_1$
a/Å	14.5103(2)	10.2518(2)	6.1478(2)	9.0270(18)
b/Å	28.8821(4)	10.4845(2)	7.5477(2)	6.2300(12)
c/Å	10.2616(1)	19.6987(4)	36.0798(1)	22.198(4)
α (°)	90	95.9376(7)	90	90
β (°)	92.184(4)	104.1553(8)	90	90
γ (°)	90	92.2975(8)	90	90
V/Å^3	4297.39(9)	2037.31(7)	1674.17(7)	1248.4(4)
Z	8	4	4	4
ρ_c/g cm^{-3}	1.068	1.107	1.259	1.241
Collected Refl.	32630	23875	4795	4269
Ind. Ref. (R_{int})	9747 (0.0601)	9270 (0.0575)	1958 (0.0476)	1399 (0.0462)
Observed Ref.	5426	5174	1312	1051
$R[I > 2\sigma(I)]$[b]	0.0634	0.0719	0.0499	0.0532
R_w (all data)[c]	0.1910	0.2251	0.1488	0.1413
$\Delta\rho_{max}$/e Å^{-3}	0.25	0.28	0.20	0.28
$\Delta\rho_{min}$/e Å^{-3}	−0.26	−0.39	−0.19	−0.28

[a] $\lambda_{Mo\text{-}K\alpha}$ = 0.7103 Å. [b] $R = \sum(F_o^2 - F_c^2)/\sum F_o^2$. [c] $R_w = [\sum w(F_o^2 - F_c^2)^2/\sum w(F_o^2)^2]^{1/2}$. [d] The OH-benzyl and 5-^{t}butyl groups of molecule **2** are disordered over two positions, with SOFs for the major components of 76% and 52%, respectively.

Table 2 Crystallographic data for compounds **5–8**

Crystal data[a]	**5**[d]	**6**	**7**	**8**[e]
Formula	$C_{10}H_{13}NO_2$	$C_{16}H_{16}N_2O_4$	$C_{16}H_{16}BrNO_2$	$C_{18}H_{21}ClN_2O_2$
MW/g mol^{-1}	179.21	300.31	334.21	332.82
Crystal system	Monoclinic	Triclinic	Triclinic	Triclinic
Space group	$P2_1/c$	$P1$	$P1$	$P\bar{1}$
a/Å	10.0724(2)	6.1083(2)	7.2044(2)	9.5103(2)
b/Å	8.2670(17)	10.3445(4)	9.3402(2)	12.8864(4)
c/Å	11.7803(2)	12.3439(5)	12.3377(3)	15.2106(4)
α (°)	90	93.254(2)	69.1986(10)	97.8703(11)
β (°)	111.75(3)	100.417(2)	80.3396(9)	107.113(1)
γ (°)	90	92.940(2)	75.9081(9)	100.4799(14)
V/Å^3	911.0(3)	764.38(5)	749.70(3)	1715.51(8)
Z	4	2	2	4
ρ_c/g cm^{-3}	1.307	1.305	1.480	1.289
Collected Refl.	3178	7278	12177	14135
Ind. Ref. (R_{int})	1596 (0.0346)	3435 (0.0517)	5691 (0.0305)	7334 (0.0393)
Observed Ref.	1186	2447	4738	4472
$R[I > 2\sigma(I)]$[b]	0.0350	0.0613	0.0432	0.0858
R_w (all data)[c]	0.1049	0.1787	0.1158	0.2786
$\Delta\rho_{max}$/e Å^{-3}	0.11	0.25	0.80	0.48
$\Delta\rho_{min}$/e Å^{-3}	−0.17	−0.23	−0.48	−0.49

[a] $\lambda_{Mo\text{-}K\alpha}$ = 0.7103 Å. [b] $R = \sum(F_o^2 - F_c^2)/\sum F_o^2$. [c] $R_w = [\sum w(F_o^2 - F_c^2)^2/\sum w(F_o^2)^2]^{1/2}$. [d] The methyl group is equally disordered over two positions (SOF = 50%). [e] The diethylamino group of the molecule **8** is disordered over two positions, SOF = 57% for the major component.

Table 3 Selected bond distances (Å) for compounds **1–7**[a]

	C2–C3	C3–C4	C4–C5	C5–C6	C6–C7	C2–C7
1a*	1.408(3)	1.388(3)	1.401(3)	1.374(3)	1.395(3)	1.403(2)
1b*	1.409(3)	1.390(2)	1.393(3)	1.375(3)	1.396(2)	1.401(3)
2a*	1.411(3)	1.384(3)	1.402(3)	1.376(3)	1.399(3)	1.403(3)
2b*	1.404(3)	1.383(3)	1.402(3)	1.369(3)	1.398(3)	1.400(3)
3*	1.386(5)	1.377(5)	1.396(5)	1.362(5)	1.396(5)	1.408(5)
4^{+}	1.416(5)	1.366(6)	1.397(6)	1.361(6)	1.405(6)	1.428(5)
5^{+}	1.415(2)	1.368(2)	1.390(2)	1.367(2)	1.412(2)	1.429(2)
6a^{+}	1.430(6)	1.346(6)	1.395(6)	1.380(5)	1.398(5)	1.441(5)
6b^{+}	1.437(6)	1.358(6)	1.407(5)	1.366(5)	1.401(5)	1.443(5)
7a^{+}	1.449(8)	1.355(7)	1.417(6)	1.364(6)	1.388(6)	1.441(6)
7b^{+}	1.443(7)	1.376(7)	1.410(7)	1.369(6)	1.390(7)	1.427(7)

[a] Two bond distances values are given when two crystallographically independent molecules are present in the asymmetric unit. Parameters correspond to (*) the enol tautomer and ($^{+}$) the keto tautomer.

In all cases, the analysis of the Fourier maps confirmed the results suggested by the IR experiments. In compounds **1–3** the H1 atom was covalently bonded to the phenol moiety and in compounds **4–7** the analysis indicated the formation of keto tautomers, with the H1 atom completely transferred to the nitrogen atom forming an enamine group.

In aromatic Schiff bases, the C2–O1 and the C8–N9 bond distances are the main structural parameters to distinguish between tautomers. For enol tautomers **1–3**, the C2–O1 bond distances were 1.349(2)/1.354(2) Å in **1a**/**1b**, 1.354(2)/1.360(2) in **2a**/**2b**, and 1.352(4) Å in **3**. While the C8═N9 bond distances are 1.268(2)/1.282(2) Å in **1a**/**1b**, 1.281(2)/1.279(2) Å in **2a**/**2b** and 1.276(4) Å in **3**. All in agreement with the reported bond distances of related phenol tautomers[25] and close to the averaged value for a C–O single bond (1.36 Å) and C═N double bonds (1.28 Å).[26] Conversely, the crystal structures of compounds **4–7** clearly showed a keto structure[27] characterized by the shortening of the C2–O1 bond distances, 1.294(5) Å in **4**, 1.314(2) Å in **5**, 1.289(5)/1.268(5) Å in **6a**/**6b** and 1.282(7)/1.286(7) Å in **7a**/**7b**.

Moreover, the C–C bond lengths of the salicylidene ring (C2–C7) in enol tautomers **1–3** showed similar values, whereas in compounds **4–7**, the bond distances reveal an alternating shortening and lengthening of the C–C bonds (Table 3). These results are in complete agreement with the assigned tautomeric forms.

Analysis of intramolecular interactions in compounds 1–7

The compounds herein reported showed two types of intramolecular hydrogen bonds, O1–H1···N9 in enol and N9–H9···O1 in the keto form. These interactions account for the formation of closely planar pseudoaromatic chelates $S(6)$.[28] Further examination of the O···N lengths in these intramolecular six-membered cycles for compounds **1–8** did not reveal a clear relationship with the tautomeric nature (A complete series of hydrogen-bonding parameters is listed in Table 4 of the ESI†). Regarding this, the well-known phenomenon called resonance-assisted hydrogen bonds (RAHBs)[29] may explain the pronounced stability of the keto tautomers in terms of π-bond cooperativity effects of the conjugated system involved.[30]

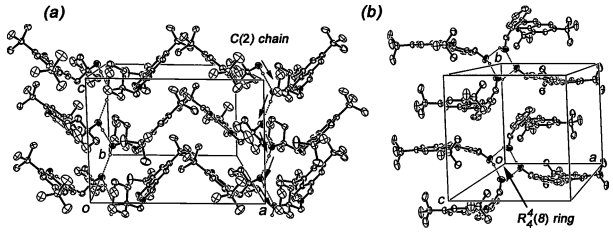

Fig. 3 Crystal packing of enol tautomers **1** (a), and **2** (b). Ellipsoids are drawn at 50% probability.

Analysis of the supramolecular arrangements for compounds 1–7

An exhaustive analysis of the structural parameters of compounds **1–7** indicated that the supramolecular structure in each tautomer is governed by one out of two intermolecular O–H···O hydrogen bonds. The O2–H2···O2 interaction, observed in the enol tautomers, associates closer molecules through aminoalcohol fragments (the aminoalcohol-aminoalcohol interaction), and the O2–H2···O1 interaction, present in keto tautomers, connects one aminoalcohol fragment with the *ortho*-hydroxy group of neighboring molecules through aminoalcohol-salicylidene interactions. Undoubtedly, the intermolecular hydrogen bonds contribute to the stabilization of the keto tautomers, which are less favored as isolated molecules.[10a,31]

A detailed examination of the supramolecular arrangements in enol tautomers **1–2** showed that only the aminoalcohol-aminoalcohol interaction (O2–H2···O2) was involved. In compound **1**, the expansion of this interaction generates infinite chains $C(2)$ of molecules along the *c* crystallographic axis (Fig. 3a), with O···O distances of 3.003(2)/3.039(2) Å in **1a**/**1b** molecules. In the case of compound **2**, this interaction promoted by the benzylic hydroxy group, led to the formation of a tetrameric ring $R_4^4(8)$ (Fig. 3b), showing O···O distances of 2.49(3)/2.78(2) Å to **2a**/**2b** molecules.

A shared characteristic of enol derivatives **1–2** is the 3,5-substitution by bulky *tert*-butyl groups that prevent the participation of the salicylidene fragment in intermolecular arrangements.

As a general trend, the ketonic salicylidene O1 atom commonly adopts the role of hydrogen-acceptor in the hydrogen-bonding geometry of the keto or zwitterionic tautomers, which is closely related to the high electrostatic charge of the heteroatoms (N and O)[4,10a] (Scheme 1).

Accordingly, in compounds **3–7**, the only hydrogen-bonding interaction in their supramolecular structures is the aminoalcohol-salicylidene (O2–H2···O1) interaction. By expanding this interaction, infinite chains $C(9)$ of molecules are generated along the *a* crystallographic axis in **3** (Fig. 4a) and along the *b* axis in **4** (Fig. 4b) and **5** (Fig. 4c). Additionally, an analogous interaction promotes the formation of a dimeric cycle $R_2^2(18)$ between two crystallographically independent molecules in imine **6** (Fig. 4d) and **7** (Fig. 4e). In compound **3**, the participation of the enolic salicylidene O1 atom in the crystal packing was attributed to the acquired conformation in the fragment of the aminoalcohol by the presence of the bulky diphenyl unit.

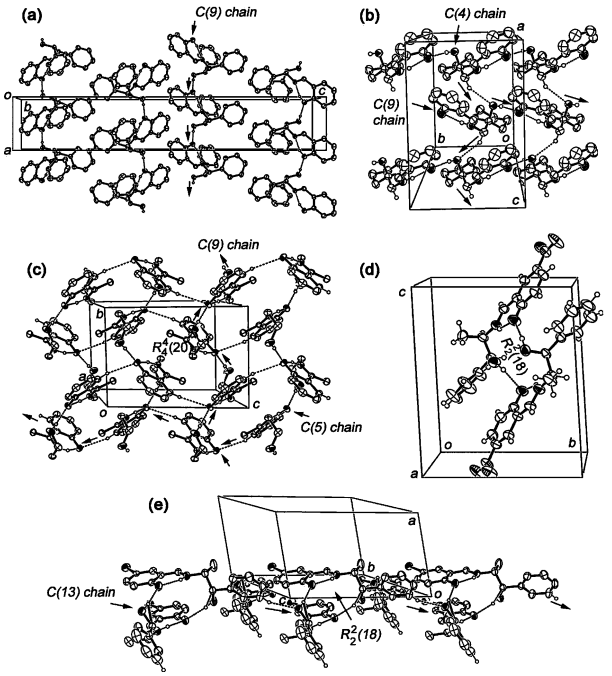

Fig. 4 Crystal packing of enol tautomer **3** (a), keto tautomers **4** (b), **5** (c), **6** (d) and **7** (e). Ellipsoids are drawn at 50% probability.

It is worth to notice that weaker C–H···O hydrogen bonds[32] complement the packing of the tautomers (with exception of **3**); however, the number in the case of the keto tautomers is larger than the one present in enol forms. In compound **4**, the C10–H10B···O2 contacts form a $C(4)$ chain of molecules that developed perpendicularly to the $C(9)$ chain established by the O2–H2···O1 interactions (Fig. 4b). In compound **5**, an expanded intramolecular ring $R_4^2(20)$ is formed by C6–H6···O1 interactions (Fig. 4c). Finally, intermolecular dimers were found in the packing of keto tautomer **7** linked through the C14B–H14B···O2A contacts, forming chains of dimers $C(13)[R_2^2(18)]$ along the *c* crystallographic axis (Fig. 4e).

In the case of the structurally related compounds **6–7**, the electronwithdrawing nature of the *para*-substituted group (NO_2 or Br) in the salicylidene fragment displaces the equilibrium exclusively to the keto form by completing proton transfer from the O1 to N9 atom. As expected, intermolecular interactions O2–H2···O1 complemented the stabilization of these keto tautomers. The O···O distances are 2.728(5)/2.725(4) Å in **6a**/**6b** and 2.721(5)/2.719(5) Å in **7a**/**7b**. Lastly, two additional Br···O contacts complete the sphere of coordination of the salicylidene O1 atom of compound **7** (ESI†).

X-Ray diffraction and solid-state NMR of compound 8

The X-ray diffraction analysis[24] of compound **8** showed that the enol (labeled as **8A**) and the keto (labeled as **8B**) tautomers cocrystallized in the unit cell in a 1 : 1 ratio (Fig. 5). The crystal structure has two intramolecular cycles $S(6)$ that result from the O1A–H1A···N9A [$d_{O1\cdots N9}$ = 2.591(4) Å] and N9B–H9B···O1B [$d_{O1\cdots N9}$ = 2.623(3) Å] interactions. Moreover, the C2–O1 and C8–N9 bond distances attained

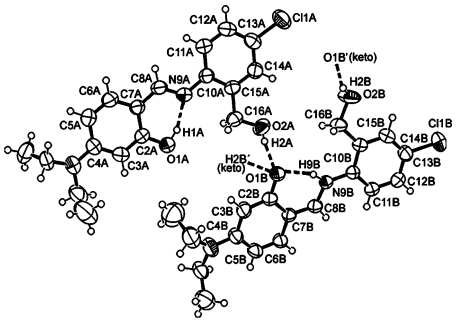

Fig. 5 ORTEP drawing of the crystal structure of **8** showing one-half of the centrosymmetric arrangement where the enol and the keto tautomers co-crystallized in the unit cell.

values of 1.335(4) Å and 1.285(4) Å in the enol **8A** and 1.303(3) Å and 1.328(3) Å in the keto form **8B**, respectively. Similar bond distances were observed by Dong *et al.* in the cocrystallization of enol and keto tautomers from aza compounds.[33]

The crystal packing of derivative **8** (Fig. 5) is characterized by a centrosymmetric arrangement including the co-crystallization of both tautomers. The O(1B) atom of the keto species plays the role of triple hydrogen-bond acceptor and two adjacent OH-benzylic groups from enol-O(2A), keto-O(2B) and the N(9B) atoms are the corresponding donors. Two keto molecules form an expanded dimeric array (not shown) $R_2^2(20)$ by means of O2B–H2B···O1B′ interaction ($d_{O2B\cdots O1B}$ = 2.702(4) Å). Furthermore, two neighboring OH-benzylic groups from enol molecules interact with keto-O(1B) atoms through O2A–H2A···O1B contacts ($d_{O2A\cdots O1B}$ = 2.735(4) Å).

As an additional evidence supporting the coexistence of the two tautomeric forms in the crystal of **8**, its ^{13}C CPMAS spectrum was obtained from the same samples studied by X-ray crystallography. Solid-state ^{13}C CPMAS NMR is a powerful technique capable of distinguishing between crystallographic entities such as polymorphs,[34] solvates and hydrates,[35] providing additional information, such as the number of molecules in the asymmetric unit.[14,36]

As noted in Fig. 6, a set of doublets of equal intensity for each expected signal confirmed the presence of two molecules per asymmetric unit. The ^{13}C CPMAS dipolar dephasing experiment (to distinguish quaternary carbon atoms by suppressing any CH and CH_2 signals) complemented the tentative assignment of the enol and keto tautomers signals. Two aromatic resonances at δ 177.7 and δ 163.6 that remained with equal intensity after the NQS experiment were assigned to C═O and C–OH carbon atoms, respectively, in agreement with known shifts for the keto and enol forms.

An analogous analysis of the solid state spectra of compounds **5–6** (see ESI†) further support our carbonyl assignments. The signal at δ = 179.5 for compound **6** corresponds to the two crystallographically independent carbonyl groups found in the asymmetric unit. Additionally, a single peak assigned to C═O at δ = 178.7 was observed in the spectrum of derivative **5** where one crystallographically independent keto molecule was present per asymmetric unit. It therefore became clear that the stabilization of the keto forms

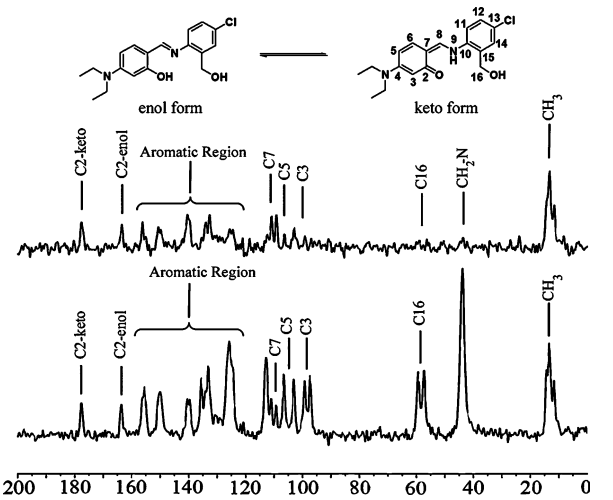

Fig. 6 Below: solid-state ^{13}C CPMAS spectra of compound **8**. Above: ^{13}C CPMAS dipolar dephasing experiment showing only quaternary and methyl carbons.

in this aggregate is enhanced by the multiple O2–H2···O1 hydrogen bonds, which are common interactions in the formation of the keto species.

Conclusions

The synthesis and the crystallographic study at room temperature of eight Schiff bases is reported. In the solid-state, each tautomer was characterized by different intermolecular O–H···O hydrogen bonds. The O2–H2···O2 interactions (aminoalcohol-aminoalcohol) were principally related to the enol forms in compounds **1** and **2**, and the O2–H2···O1 interactions (aminoalcohol-salicylidene) were fundamentally associated with the keto species in compounds **4–7**. Although, the enol tautomer was also observed in the case of derivative **3**, voluminous substituents (*i.e.* diphenyl unit in the side of the aminoalcohol) prevent the formation of the expected O2–H2···O2 bonds and force the formation of O2–H2···O1 interactions. Additionally, the co-existence in the solid-state of both the keto and enol tautomers in **8** was supported by X-ray diffraction and solid-state NMR experiments. Solution UV-Vis experiments and solution VT NMR studies clearly revealed that the predominance for one tautomer is strongly dependent on the solvent investigated and the temperature used. Keto forms are preferred in protic solvents whereas enol tautomers were observed in aprotic ones. In spite of that, the preferential formation of a particular tautomer in the solid state is modulated through a combination of the steric factors of the substituents modifying the consequent capability of the molecules to interact with each other through appropriate intermolecular O–H···O hydrogen bonds.

Experimental

Melting points were obtained with an Electrothermal 9200 apparatus and are uncorrected. Infrared spectra were measured on a FTIR Varian spectrophotometer ATR. ^{1}H and ^{13}C spectra as well as Correlation Spectroscopy ^{1}H-^{1}H COSY and Heteronuclear Chemical Shift Correlation ^{1}H-^{13}C HETCOR were recorded on JEOL eclipse +400 and ECA +500 spectrometers. Chemical shifts (ppm) are relative to $(CH_3)_4Si$ for ^{1}H and ^{13}C. Mass spectra were recorded on an Agilent G1969A APCI Atmospheric Pressure-Chemical Ionization time-of-flight spectrometer. UV-Vis spectra were recorded on a Perkin Elmer Lambda 900 spectrophotometer.

Solid-state NMR experiments

Crystalline samples of selected compounds obtained from methanolic solutions were previously ground with a mortar and a pestle at room temperature in order to get homogeneity, and they were packed in a 4 mm wide ZrO_2 rotor with a KelF cap using 80–90 mg of each compound. ^{13}C CPMAS solid state NMR spectra of selected compounds were obtained on a Bruker AVANCE II300 spectrometer operating at ^{13}C frequency of 75.47 MHz with ^{1}H broadband decoupler using a 4 mm broadband probe. A spinning frequency of 10 kHz at the magic angle was found to be successful for the removal of spinning sidebands using an optimized cross polarization contact time of 1 ms. Dipolar dephasing experiments (^{13}C CPMAS non-quaternary suppression) were carried out with a delay of 25 μs before turning the ^{1}H decoupler on.

Single crystal X-ray structure determinations

All diffraction data were measured using an Enraf Nonius Kappa-CCD diffractometer with graphite-monochromated $\lambda_{Mo\text{-}K\alpha}$ = 0.71073 Å. Frames were collected at T = 293 K *via* ω/φ rotation. Direct methods SHELXS-86 and SIR-2004 were used for structure solution and SHELXL-97 program package for refinement and data output.[24] C–H hydrogen atoms were placed in geometrically calculated positions using a riding model. O–H and N–H hydrogen atoms have been localized by difference Fourier maps and their bond distances and isotropic temperature factors have been refined freely (In compound **3**, one restraint was necessary to fix a long O1–H1 bond distance [1.16(4) Å] with a DFIX 0.84 instruction). Three and four restraints were automatically inserted by SHELXL to fix the origin of the lattice in the refinement of compounds **6** and **7**, respectively. Fifteen restraints were required to make the C–N and C–C bond distances of the diethylamino groups identical (one of them disordered over two positions) of the two crystallographically independent molecules of compound **8**. As indicated in the literature,[37] in compounds **3**, **4** and **6** the Friedel opposites were merged before final refinement (MERG 4). The absolute configuration of **3** and **6** was chosen on the basis of the known configuration of the starting materials, while the configuration of **4** was arbitrarily selected. The Flack parameter for compound **7** refined satisfactorily to 0.028(9). Figures were created with ORTEP-3 for windows version 2.02. Verification of hydrogen-bonding interactions in the crystal lattice was carried out with PLATON program under the WINGX interface.

Acknowledgements

The authors thank CONACyT (project No. 83519) and UNAM (PAPIIT IN-214010) for financial support and the scholarship to O. Domínguez and B. Rodríguez-Molina.

Thanks are given to Consejo Superior de la Investigación Científica en España for the Cambridge Crystallographic Data Base license, to M. L. Rodríguez and V. González for NMR spectra, G. Cuéllar for MS, M. A. Leyva for X-ray diffraction and Dr E. García-Báez for valuable discussion.

Notes and references

1 (*a*) Y. Gat and M. Sheves, *J. Am. Chem. Soc*., 1993, **115**, 3772–3773; (*b*) S. Ren, R. Wang, K. Komatsu, P. Bonaz-Krause, Y. Zyrianov, C.-E. McKenna, C. Csipke, Z. A. Tokes and E. J. Lien, *J. Med. Chem*., 2002, **45**, 410–419.

2 (*a*) G. K. Patra and I. Goldberg, *Cryst. Growth Des*., 2003, **3**, 321–329; (*b*) M. Sliwa, S. Létard, I. Malfant, M. Nierlich, P. G. Lacroix, T. Asahi, H. Masuhara, P. Yu and K. Nakatani, *Chem. Mater*., 2005, **17**, 4727–4735; (*c*) M. Sliwa, A. Spangenberg, I. Malfant, P. G. Lacroix, R. Métivier, R. B. Pansu and K. Nakatani, *Chem. Mater*., 2008, **20**, 4062–4068; (*d*) E.-Q. Gao, Y.-F. Yue, S.-Q. Bai, Z. He and C.-H. Yan, *Cryst. Growth Des*., 2005, **5**, 1119–1124.

3 (*a*) C. D. Meyer, C. S. Joiner and J. F. Stoddart, *Chem. Soc. Rev*., 2007, **36**, 1705–1723; (*b*) M.-D. Zhou, J. Zhao, J. Li, S. Yue, C.-N. Bao, J. Mink, S. L. Zang and F. E. Kühn, *Chem.–Eur. J*., 2007, **13**, 158–166; (*c*) R. M. Moreno, M. Rosol and A. Moyano, *Tetrahedron: Asymmetry*, 2006, **17**, 1089–1103.

4 (*a*) V. Jeseentharani, J. Selvakumar, A. Dayalan, B. Varghese and K.-S. Nagaraja, *J. Mol. Struct*., 2010, **966**, 122–128; (*b*) K. Ogawa, J. Harada, I. Tamura and Y. Noda, *Chem. Lett*., 2000, 528–529; (*c*) S. Bilge, Z. Kiliç, Z. Hayvali, T. Hökelek and S. Safran, *J. Chem. Sci*., 2009, **121**, 989–1011.

5 (*a*) J. L. Scott and K. Tanaka, *Cryst. Growth Des*., 2005, **5**, 1209–1213; (*b*) J. Harada, H. Uekusa and Y. Ohashi, *J. Am. Chem. Soc*., 1999, **121**, 5809–5810; (*c*) E. Hadjoudis and I.-M. Mavridis, *Chem. Soc. Rev*., 2004, **33**, 579–588.

6 (*a*) H. Tian and S. Yang, *Chem. Soc. Rev*., 2004, **33**, 85–97; (*b*) F. M. Raymo and S. Giordano, *Org. Lett*., 2001, **3**, 3475–3478; (*c*) L. Giordano, T. M. Jovin, M. Irie and E. A. Jares-Erijman, *J. Am. Chem. Soc*., 2002, **124**, 7481–7489; (*d*) S. J. Lim, J. W. Seo and S. Y. Park, *J. Am. Chem. Soc*., 2006, **128**, 14542–14547; (*e*) J. L. Maldonado, Y. Pónce-de-Léon, G. Ramos-Órtiz, M. Rodríguez, M. A. Meneses-Nava, O. Barbosa-García, R. Santillan and N. Farfán, *J. Phys. D: Appl. Phys*., 2009, **42**, 075102; (*f*) H. Fukuda, K. Amimoto, H. Koyama and T. Kawato, *Org. Biomol. Chem*., 2003, **1**, 1578–1583.

7 (*a*) P.-E. Hansen, Z. Rozwadowski and T. Dziembowska, *Curr. Org. Chem*., 2009, **13**, 194–215; (*b*) R. M. Claramunt, C. López, M.-D. Santa María, D. Sanz and J. Elguero, *Prog. Nucl. Magn. Reson. Spectrosc*., 2006, **49**, 169–206; (*c*) Y.-M. Hijji, B. Barare, A.-P. Kennedy and R. Butcher, *Sens. Actuators, B*, 2009, **136**, 297–302; (*d*) A. Perona, D. Sanz, R. M. Claramunt and J. Elguero, *Molecules*, 2006, **11**, 453–463; (*e*) J. H. Chong, M. Sauer, B. O. Patrick and M. J. MacLachlan, *Org. Lett*., 2003, **5**, 3823–3826; (*f*) E. Ito, H. Oji, T. Araki, K. Oichi, H. Ishii, Y. Ouchi, T. Ohta, N. Kosugi, Y. Maruyama, T. Naito, T. Inabe and K. Seki, *J. Am. Chem. Soc*., 1997, **119**, 6336–6344.

8 (*a*) A. Özek, Ç. Albayrak, M. Odabaoğlu and O. Büyükgüngör, *Acta Crystallogr., Sect. C: Cryst. Struct. Commun*., 2007, **63**, o177–180; (*b*) C. C. Ersanli, M. Odabaoğlu, Ç. Albayrak and A. Erdönmez, *Acta Crystallogr., Sect. E: Struct. Rep. Online*, 2004, **60**, o264–266.

9 (*a*) C.-J. Chang, T.-L. Shieh and H. G. Floss, *J. Med. Chem*., 1977, **20**, 176–178; (*b*) W. Schilf, B. Kamieńsky and T. Dziembowska, *J. Mol. Struct*., 2002, **602–603**, 41–47; (*c*) S. Sharif, G. S. Denisov, M. D. Toney and H.-H. Limbach, *J. Am. Chem. Soc*., 2006, **128**, 3375–3387; (*d*) Z. Rozwadowski and T. Dziembowska, *Magn. Reson. Chem*., 1999, **37**, 274–278.

10 (*a*) K. Ogawa and J. Harada, *J. Mol. Struct*., 2003, **647**, 211–216; (*b*) Filarowski, A. Kochel, M. Kluba and F. S. Kamounah, *J. Phys. Org. Chem*., 2008, **21**, 939–944; (*c*) M. Sauer, C. Yeung, J. H. Chong, B. O. Patrick and M. J. MacLachlan, *J. Org. Chem*., 2006, **71**, 775–788.

11 M. Rodríguez, R. Santillan, Y. López, N. Farfán, V. Barba, K. Nakatani, E. V. García-Baez and I. I. Padilla-Martínez, *Supramol. Chem*., 2007, **19**, 641–653.

12 K. Ogawa, Y. Kasahara, Y. Ohtani and J. Harada, *J. Am. Chem. Soc*., 1998, **120**, 7107–7108.

13 (*a*) K. Ogawa, J. Harada, T. Fujirawa and S. J. Yoshida, *J. Phys. Chem. A*, 2001, **105**, 3425–3427; (*b*) T. Fujiwara, J. Harada and K. Ogawa, *J. Phys. Chem. A*, 2009, **113**, 1822–1826.

14 (*a*) L. Antonov, W. M. F. Fabian, D. Nedeltcheva and F. S. Kamounah, *J. Chem. Soc., Perkin Trans. 2*, 2000, 1173–1179; (*b*) M. Kluba, P. Lipkowski and A. Filarowski, *Chem. Phys. Lett*., 2008, **463**, 426–430; (*c*) T. Dziembowska, M. Szafran, A. Katrusiak and Z. Rozwadowski, *J. Mol. Struct*., 2009, **929**, 32–42.

15 (*a*) A. Koll and P. Wolschann, *Monatsh. Chem*., 1996, **127**, 475–486; (*b*) A. Filarowski, T. Glowiak and A. Koll, *J. Mol. Struct*., 1999, **484**, 75–89; (*c*) A. Filarowski, A. Koll and T. Glowiak, *Monatsh. Chem*., 1999, **130**, 1097–1108.

16 (*a*) M. Miura, J. Harada and K. Ogawa, *J. Phys. Chem. A*, 2007, **111**, 9854–9858; (*b*) R. Herzfeld and P. Nagy, *Curr. Org. Chem*., 2001, **5**, 373–394; (*c*) S. H. Alarcon, A. C. Olivieri, R. M. Cravero, G. Labadie and M. J. Gonzáles-Sierra, *J. Phys. Org. Chem*., 1995, **8**, 713–720.

17 (*a*) J. Jánsky and A. Koll, *Struct. Chem*., 2004, **15**, 353–361; (*b*) W. M. F. Fabian, L. Antonov, D. Nedeltcheva, F. S. Kamounah and P. J. Taylor, *J. Phys. Chem. A*, 2004, **108**, 7603–7612.

18 (*a*) A. Filarowski, A. Koll, M. Rospenk and I. Krol-Starzomska, *J. Phys. Chem. A*, 2005, **109**, 4464–4473; (*b*) N. Wachter-Jurcsak and C. A. Detmer, *Org. Lett*., 1999, **1**, 795–798.

19 (*a*) I. Król-Starzomska, A. Filarowski, M. Rospenk, A. Koll and S. Melikova, *J. Phys. Chem. A*., 2004, **108**, 2131–2138; (*b*) T. Dziembowska, Z. Rozwadowski, A. Filarowski and P. E. Hansen, *Magn. Reson. Chem*., 2001, **39**, S67–S80.

20 (*a*) P. Gilli, V. Bertolasi, V. Ferretti and G. Gilli, *J. Am. Chem. Soc*., 2000, **122**, 10405–10417; (*b*) P. Gilli, V. Bertolasi, L. Pretto, L. Antonov and G. Gilli, *J. Am. Chem. Soc*., 2005, **127**, 4943–4953.

21 A. Filarowski and I. Majerz, *J. Phys. Chem. A*, 2008, **112**, 3119–3126.

22 (*a*) N. S. Golubev, S. N. Smirnov, P. M. Tolstoy, S. Sharif, M. D. Toney, G. S. Denisov and H. H. Limbach, *J. Mol. Struct*., 2007, **844–845**, 319–227; (*b*) X. C. Tang, M. J. Pikal and L. S. Taylor, *Pharm. Res*., 2002, **19**, 484–490.

23 (*a*) J. W. J. Ledbetter, *J. Phys. Chem*., 1977, **81**, 54–59; (*b*) G. Wojciechowski, P. Przybylski, W. Schilf, B. Kamieński and B. Brzezinski, *J. Mol. Struct*., 2003, **649**, 197–205; (*c*) V. P. Rybalkin, A. D. Dubonosov, E. N. Shepelenko, L. L. Popova, M. I. Makarova, A. V. Tsukanov, B. A. Bren' and V. I. Minkin, *Russ. J. Org. Chem*., 2002, **38**, 1326–1330.

24 Structure solution: (*a*) G. M. Sheldrick, *SHELXS-86—Program for crystal structure solution*, University of Göttingen, Germany, 1986; (*b*) M. C. Burla, R. Caliandro, M. Camalli, B. Carrozzini, G. L. Cascarano, L. De Caro, C. Giacovazzo, G. Polidori and R. Spagna, *J. Appl. Crystallogr*., 2005, **38**, 381–388; (*c*) Data Refinement: G. M. Sheldrick, *SHELXL-97—Program for the refinement of crystal structure*, University of Göttingen, Germany, 1997; (*d*) ORTEP-Graphics: L. Farrugia, *J. Appl. Crystallogr*., 1997, **30**, 565; (*e*) PLATON-Hydrogen bonding interactions: A. L. Spek, *J. Appl. Crystallogr*., 2003, **36**, 7–13; (*f*) WINGX-interface: L. Farrugia, *J. Appl. Crystallogr*., 1999, **32**, 837–838.

25 (*a*) V. T. Kasumov, H. Türkmen, İ. Uçar, A. Bulut and N. Yaylı, *Spectrochim. Acta, Part A*, 2008, **70**, 60–68; (*b*) A. Takashiro and E. Yasuaki, *Acta Crystallogr., Sect. E: Struct. Rep. Online*, 2006, **62**, o4315–4317.

26 F. H. Allen, O. Kennard, D. G. Watson, L. Brammer, A. G. Orpen and R. Taylor, *Typical Interatomic Distances: Organic Compounds in International Tables of Crystallography*, IUCR, 1992, vol. C, pp. 790–811.

27 (*a*) X.-X. Sun, S.-L. Ma, H. B. Huang and C.-M. Qi, *Acta Crystallogr., Sect. C: Cryst. Struct. Commun*., 2007, **63**, o87–88; (*b*) B. Kaitner and G. Pavlović, *Acta Crystallogr., Sect. C: Cryst. Struct. Commun*., 1996, **52**, 2573–2575.

28 For hydrogen-bond motifs notations see: J. Bernstein, R. E. Davis, L. Shimoni and N.-L. Chang, *Angew. Chem., Int. Ed. Engl*., 1995, **34**, 1555–1573.

29 (*a*) P. Gilli, V. Bertolasi, L. Pretto, V. Ferreti and G. Gilli, *J. Am. Chem. Soc*., 2004, **126**, 3845–3855; (*b*) V. Bertolasi, P. Gilli, V. Ferretti and G. Gilli, *J. Am. Chem. Soc*., 1991, **113**, 4917–4925.
30 V. Bertolasi, L. Pretto, G. Gilli and P. Gilli, *Acta Crystallogr., Sect. B: Struct. Sci*., 2006, **62**, 850–863.
31 (*a*) S. D. Chatziefthimiou, Y. G. Lazarou, E. Hadjoudis, T. Dziembowska and I. M. Mavridis, *J. Phys. Chem. B*, 2006, **110**, 23701–23709; (*b*) K. Pyta, P. Przybylski, W. Schilf, B. Kołodziej, A. Szady-Chełmieniecka, E. Grech and B. Brzezinski, *J. Mol. Struct*., 2010, **967**, 140–166.
32 (*a*) T. Steiner, *Crystallogr. Rev*., 1996, **6**, 1–57; (*b*) G. R. Desiraju, *Acc. Chem. Res*., 1991, **24**, 290–296; (*c*) P. A. Wood, F. H. Allen and E. Pidcock, *CrystEngComm*, 2009, **11**, 1563–1571.
33 Z.-H. Wu, J.-P. Ma, X.-W. Wu, R.-Q. Huang and Y.-B. Dong, *Acta Crystallogr., Sect. C: Cryst. Struct. Commun*., 2009, **65**, o128–130.
34 (*a*) R. K. Harris, *J. Pharm. Pharmacol*., 2007, **59**, 225–239; (*b*) M. R. Caira, *Top. Curr. Chem*., 1998, **198**, 163–208.
35 (*a*) S. M. Reutzel-Edens, J. K. Bush, P. A. Magee, G. A. Stephenson and S. R. Byrn, *Cryst. Growth Des*., 2003, **3**, 897–907; (*b*) G. A. Stephenson, J. G. Stowell, P. H. Toma, R. R. Pfeiffer and S. R. Byrn, *J. Pharm. Sci*., 1997, **86**, 1239–1244.
36 R. K. Harris, S. A. Joyce, C. J. Pickard, S. Cadars and L. Emsley, *Phys. Chem. Chem. Phys*., 2006, **8**, 137–143.
37 (*a*) H. D. Flack and G. Bernardinelli, *J. Appl. Crystallogr*., 2000, **33**, 1143–1148; (*b*) A. Białosńka and Z. Ciunik, *Acta Crystallogr., Sect. C: Cryst. Struct. Commun*., 2007, **63**, o120–o122.

